

APPENDIX

C. EXAMPLES OF DYNAMICAL EFFECTS

To demonstrate some capabilities of our N-body model we present several numerical simulations that can be treated as examples of what can be fitted to observational data (more examples can be found in Fabrycky 2010).

C.1. *Precession of ω and Ω*

Probably the most trivial perturbation is the precession of the argument of pericentre ω . In our case however, the temporal derivative $\dot{\omega}$ is *not* a free parameter; it is directly tied to the masses and initial osculating elements of the bodies. The same holds for the longitude of the ascending node Ω and the corresponding $\dot{\Omega}$. It is thus not necessary to use any secular theories, because all secular perturbations are implicitly included in our N-body model. Moreover, one can expect that neither $\dot{\omega}(t)$ nor $\dot{\Omega}(t)$ are exactly constant, because some short-periodic perturbations are always present.

Depending on the distribution of the angular momentum \mathbf{L} in the system, the precession of individual orbits can occur with different amplitudes, although the secular time scales for a pair of orbits are the same. In the Laplace coordinate system (aligned with total \mathbf{L}), all $\bar{\omega}_j$ and $\bar{\Omega}_j$ circulate from 0 to 360°. On the other hand, our frame of reference is tied to the observers direction and the sky plane, so that ω_j or Ω_j often *librate*, in other words oscillate in a limited interval, due to the purely geometrical projection.

Apart from the above basic secular perturbations, we also account for an additional precession caused by tides, oblateness and general-relativistic effects (Eqs. (2) to (4)).

C.2. *Inclination vs eclipse durations*

As a result of the nodal precession $\dot{\Omega}_j$ of each orbit, the inclinations i_j with respect to the sky plane also often librate. Regarding the case of i_1 , the eclipsing binary may exhibit one or more

photometric effects: changes of eclipse durations, eclipse depths, or completely disappearing (and later reappearing) eclipses. All of these are accounted for and contribute to χ_{ecl}^2 , χ_{lc}^2 , or χ_{ttv}^2 terms.

Our model is also extremely sensitive to the *mutual* inclination J of the orbits, because the precession rates are functions of it (see Eqs. 26 and 27 in Nemravová et al. 2016, but these are suitable only for low e_1 , low J and large a_2/a_1). This may significantly contribute to χ_{sky}^2 , or χ_{vis}^2 .

C.3. *Eccentricity oscillations*

Yet another phenomenon may occur on secular time scales, namely oscillations of the osculating eccentricity $e_1(t)$ forced by the 3rd body. In an 'extreme' case, $e_1(t = T_0) \simeq 0.1$, it is manifested as forced oscillations of radial velocities which no longer have constant amplitudes.

For low eccentricities of the order of 0.01, one can search for some phase shifts of RVs of components 1 and 2. This turns out to be a strong constraint for the initial eccentricity $e_1(t = T_0)$, because the phase shifts occur as soon as $e_1 \neq 0$. An example for ξ Tau system is shown in Figure ??.

C.4. *Kozai cycles*

A closely related classical example are the Kozai cycles (Kozai 1962, Lidov 1962), or *coupled* oscillations of the eccentricity e and mutual inclination J which preserve the invariant $L_z = \sqrt{1 - e^2} \cos J$. They occur for high-inclination orbits with a certain minimum (critical) inclination J_{min} .

We can easily demonstrate such oscillations, if we substantially increase the mutual inclination J in ξ Tau system (see Figure C1). However, in this particular case the system is so massive and compact that the approximations involved in the derivation of L_z integral do not hold anymore! The respective time scale (19 yr) of the oscillations is also much shorter than predicted by the analytical theory; and there is a 4th body with a 51 yr orbit involved, so that the phasing of e , i is not exact.

For compact systems it is worth to verify if tides or oblateness are capable of suppressing Kozai oscillations or not by enforcing a different precession rate (for a reasonably high value of k_L , i.e. $\simeq 0.3$

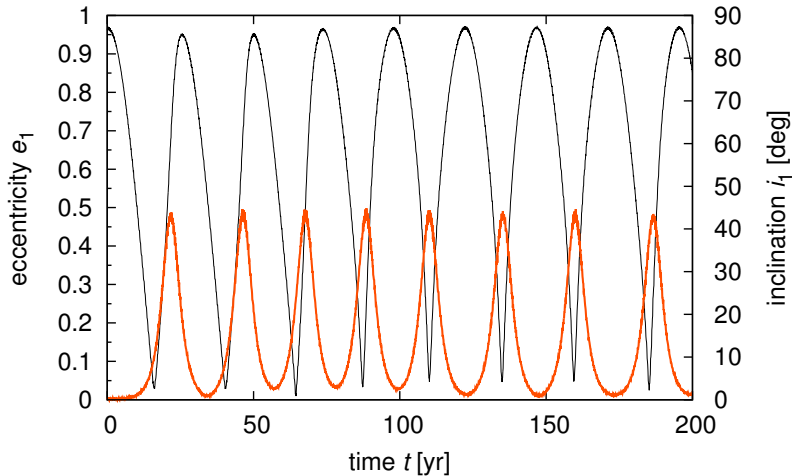


Figure C1. The Kozai cycles in a hypothetical quadruple system with the mutual inclination $J = 50^\circ$ of the first two orbits, i.e. larger than the critical value J_{\min} . The coupled oscillations of the eccentricity e_1 (orange) and inclination i_1 (black) would be visible, on the time scale as short as $T_{\text{Kozai}} \simeq 19 \text{ yr}$. Note in this case tides or oblateness are *not* strong enough to suppress these oscillations (cf. Fabrycky 2010), when we assume the Love number $k_L = 0.3$.

for M dwarfs, or as small as 10^{-2} for solar-like stars; Mardling & Lin 2004).

C.5. Variation and evection

Leaving secular perturbations aside, there are short-periodic perturbations which occur on the *orbital* time scales P_j of individual orbits. In a classical Hills theory, we would have five terms contributing to departures of the true longitude $\Delta\lambda$ (Fitzpatrick 2012): eccentricity, ellipticity, inclination, variation and evection. The last two are of interest, as they arise from interactions with an external 3rd body. One can recognise the variation is maximal in octant points, and the evection in quadrant points (wrt. to the 3rd body).

In Figure C2 we demonstrate these short-periodic effects for a system similar to ξ Tau. Note the 3rd body may be virtually ‘fixed’ and still cause variation or evection which contribute mostly to χ_{rv}^2 , but not directly to χ_{ttv}^2 , since the eclipses are always measured at the same true longitude λ .

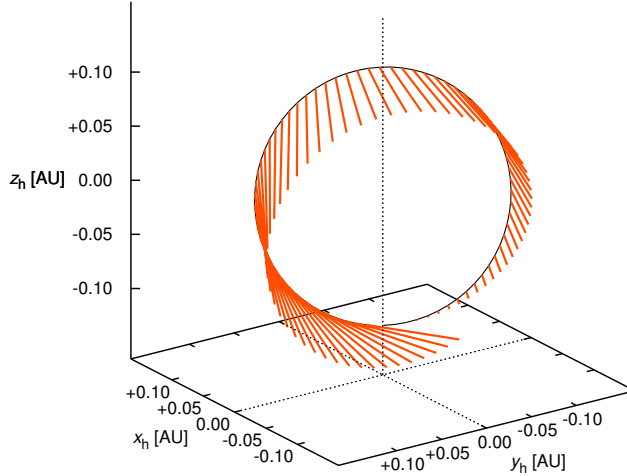


Figure C2. A general trajectory of the inner eclipsing binary as output from our N-body model, affected by the 3rd and 4th component in ξ Tauri quadruple system. The differences (orange lines) with respect to a keplerian orbit (black curve) — fixed at the initial conditions — were exaggerated 100 times to make them visible at all. Two most important terms describing departures in longitude $\Delta\lambda$ are called the variation and evection. Alternatively, the keplerian orbit could have been optimized, so that $\Delta\lambda$ are smaller at certain λ , but never zero everywhere.

C.6. *Prograde vs retrograde orbits*

Traditionally, it is practically impossible to distinguish prograde and retrograde orbits, because the corresponding RVs are the same. But luckily, mutual interactions within the N-body model can contribute to χ_{ttv}^2 sufficiently (cf. Fig. 12 in Nemravová et al. 2016). The principle is as follows: if the distance of the 3rd body is increasing (or decreasing) during one P_1 , the gravitational potential at around the binary is less negative (or more) and consequently the value of P_1 is inevitably larger (smaller).

C.7. *Long-term evolution and stability*

It is also possible to run the N-body integrator separately, regardless of an observational time span, and study a long-term evolution and stability of stellar systems. We may wish to prefer those orbital solutions which are indeed stable.

One of the difficulties is that the output of osculating elements is either prohibitively long or an

aliasing occurs when the output time step Δt_{out} is larger than an half of the shortest orbital period, $P_1/2$ (cf. Figure C3, top).

In a modified version of the BS integrator (`swift_bs_fp`), we can use an on-line digital filtering of non-singular osculating elements h_j, k_j, p_j, q_j to overcome these problems: first a multi-level convolution based on the Kaiser windows (Quinn et al. 1991) to obtain *mean* elements, and second a frequency-modified Fourier transform (Šidlichovský & Nesvorný 1997) to extract *proper* elements. For N mutually interacting bodies, one can expect $2N$ eigen-frequencies of the system, which are usually denoted g_j and s_j . The corresponding amplitudes e_{pj} , $\sin \frac{1}{2} I_{pj}$ can be considered approximate integrals of motion which only evolve on time scales longer than secular (see Figure C3, bottom).

C.8. *Close encounters*

Additionally, one can model hyperbolic trajectories and three-body encounters or captures, even though from a historical perspective such stellar models do not seem very convincing (Tokovinin 1986), because some observations might have been affected by raw measurement errors (e.g. a wrong plate scale), an abrupt change of the orbital period may turn out to be rather quasiperiodic (possibly related to magnetic phenomena) and any inter-stellar encounter is considered an exceedingly rare event.

Finally, let us mention that all mean-motion resonances (Rivera et al. 2005), secular resonances, three-body resonances (Nesvorný and Morbidelli 1998), or chaotic diffusion due to overlapping resonances are also naturally accounted for in our N-body model.

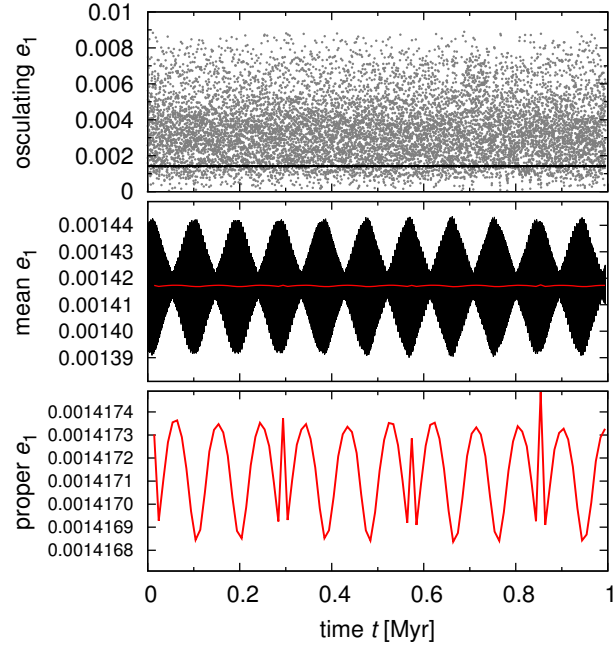


Figure C3. A long-term evolution of ξ Tauri quadruple system, or the eccentricity $e_1(t)$ of the 1st orbit, respectively. There are osculating (top), mean (middle), and proper (bottom) orbital elements shown. Note the osculating elements may exhibit *aliasing*, i.e. artificial long-period changes, because the output time step $\Delta t_{\text{out}} = 100$ yr is too long and the corresponding Nyquist period is $P_{\text{Ny}} = \Delta t_{\text{out}}/2$. The mean elements were computed with the following setup: input sampling $\Delta t = 3$ d, sequence of filters denoted A, A, A, and B (from Quinn et al. 1991), with decimation factors 10, 10, 10, 3, output sampling $\Delta t_{\text{mean}} = 24.6$ yr, so that the passband $P > 164.271$ yr, the total ripple at most 10^{-4} , the stopband $P < 54.757$ yr, and a minimum suppression of 10^{-9} . The proper elements were then computed from $N_{\text{samples}} = 512$, after every $\Delta t_{\text{proper}} = 10^4$ yr. There might be some minor glitches, arising from frequency peak splittings, but with very low amplitude.